

# Synthesis And Characterization Of Insulating $\text{Bi}_{0.8}\text{Pb}_{0.2}\text{Fe}_{0.9}\text{Nb}_{0.1}\text{O}_3$ (BF-0.2PFN) Multiferroic Material

Jay Prakash Patel

Department of Physics, Government Post Graduate College Musafirkhna Amethi Uttar Pradesh India Pin-227813

**Abstract:** The  $\text{Bi}_{0.8}\text{Pb}_{0.2}\text{Fe}_{0.9}\text{Nb}_{0.1}\text{O}_3$  sample is synthesized by solid state reaction method. The small trace of  $\text{LiCO}_3$  was doped for increasing the resistivity of sample during the synthesis process. The analysis of XRD pattern confirms the rhombohedral crystal structure with R3c space group for this sample. The dielectric and hysteresis loop measurements confirm the insulating properties of  $\text{Bi}_{0.8}\text{Pb}_{0.2}\text{Fe}_{0.9}\text{Nb}_{0.1}\text{O}_3$ . The magnetic transition temperature is also confirmed by the temperature dependence plot of dielectric constant.

**1. Introduction:** The materials in which ferroelectric and magnetic order parameters are simultaneously co-exist and cross coupled are called magnetoelectric multiferroic [1-6]. They have enormous applications in making of multistate memory devices, sensors, spin wave amplifiers and spintronics based devices [1-6]. The pure  $\text{BiFeO}_3$  (BF) ( $T_N \sim 643$  K,  $T_C \sim 1103$  K) and  $\text{BiFeO}_3$  based doped multiferroic systems are only discovered multiferroics in which ferroelectric and magnetic order parameters co-exist above room temperature [7-8]. The room temperature multiferroic properties of  $\text{BiFeO}_3$  and  $\text{BiFeO}_3$  doped systems make it unique materials for the designing of modern electronics devices [9-12]. The synthesis of insulating  $\text{BiFeO}_3$  is very difficult because it shows hopping conductivity due to presence of  $\text{Fe}^{3+}$  and  $\text{Fe}^{2+}$  ions and oxygen vacancies in sintered  $\text{BiFeO}_3$ . In the present study, I doped  $\text{BiFeO}_3$  with another fascinating low temperature multiferroic  $\text{Pb}(\text{Fe}_{0.5}\text{Nb}_{0.5})\text{O}_3$  (PFN) ( $T_N \sim 143$  K,  $T_C \sim 385$  K). I have selected Bismuth ferrite rich BF-0.2PFN ( $\text{Bi}_{0.8}\text{Pb}_{0.2}\text{Fe}_{0.9}\text{Nb}_{0.1}\text{O}_3$ ) composition for present study. I have synthesized insulating  $\text{Bi}_{0.8}\text{Pb}_{0.2}\text{Fe}_{0.9}\text{Nb}_{0.1}\text{O}_3$  composition by doping small trace of  $\text{Li}_2\text{CO}_3$ . In this paper, I have discussed the different steps of synthesis of insulating  $\text{BiFeO}_3$  based doped multiferroic materials  $\text{Bi}_{0.8}\text{Pb}_{0.2}\text{Fe}_{0.9}\text{Nb}_{0.1}\text{O}_3$  and their characterizations by using X-ray diffractometer (XRD), Differential scanning calorimeter (DSC), Hysteresis loop tracer and dielectric measurements.

I, present the details of synthesis of phase pure  $\text{Bi}_{0.8}\text{Pb}_{0.2}\text{Fe}_{0.9}\text{Nb}_{0.1}\text{O}_3$  solid solutions systems by solid state reaction method. The synthesis of pure  $\text{BiFeO}_3$  has been continuing a challenge because easily formation of unwanted impurity phases  $\text{Bi}_2\text{Fe}_4\text{O}_9$  [13, 14] Kumar et al. (2000)],  $\text{Bi}_{25}\text{FeO}_{39}$  [15, 16] and  $\text{Bi}_{36}\text{Fe}_2\text{O}_{57}$  [17] during their calcinations and sintering processes. On the other hand, the formation of unwanted pyrochlore phases e.g.  $\text{Pb}_3\text{Nb}_4\text{O}_{13}$  and  $\text{Pb}_2\text{Nb}_2\text{O}_7$  [18, 19] during the synthesis of  $\text{Pb}(\text{Fe}_{0.5}\text{Nb}_{0.5})\text{O}_3$  makes it more difficult to synthesize phase pure  $\text{Bi}_{0.8}\text{Pb}_{0.2}\text{Fe}_{0.9}\text{Nb}_{0.1}\text{O}_3$  samples. The  $\text{Bi}_2\text{Fe}_4\text{O}_9$  (Bi-deficient) and  $\text{Bi}_{25}\text{FeO}_{39}$ ,  $\text{Bi}_{36}\text{Fe}_2\text{O}_{57}$  (Bi-excess impurities) are formed during the calcinations stage. These impurities are controlled by optimizing the calcinations temperature and time. There was no impurity phases formed during the calcinations of the  $\text{Bi}_{0.8}\text{Pb}_{0.2}\text{Fe}_{0.9}\text{Nb}_{0.1}\text{O}_3$  compositions. The sintering of  $\text{Bi}_{0.8}\text{Pb}_{0.2}\text{Fe}_{0.9}\text{Nb}_{0.1}\text{O}_3$  pellets were carried out in the closed alumina crucibles. The powders of same compositions are used as a spacer powder to control the evaporation of Bi during the sintering.

X-ray diffractometer is a powerful instrument used to characterize and identify the different phases present in any material. The simplicity and advantage of X-ray powder diffraction method can be given as follows (i) the powder diffraction pattern is characteristic of a given substance, (ii) each substance in a mixture produces its own pattern independent of others and (iii) the method is capable of quantitative and qualitative analysis of the phases present in a given mixture. In the present case, the calcined and sintered powders were characterized for the presence of different phases in the  $\text{Bi}_{0.8}\text{Pb}_{0.2}\text{Fe}_{0.9}\text{Nb}_{0.1}\text{O}_3$  composition synthesized during this thesis work. X-ray diffraction (XRD) measurements were carried out using an 18 kW rotating anode ( $\text{CuK}\alpha$ ) based Rigaku (RINT 2000/PC series) powder diffractometer operating in the Bragg-Brentano geometry and fitted with a graphite monochromator in the diffracted beam.

**2. Synthesis of  $\text{Bi}_{0.8}\text{Pb}_{0.2}\text{Fe}_{0.9}\text{Nb}_{0.1}\text{O}_3$  (BF-0.2PFN):**  $\text{Bi}_{0.8}\text{Pb}_{0.2}\text{Fe}_{0.9}\text{Nb}_{0.1}\text{O}_3$  was synthesized through conventional solid state reaction route. The conditions and sequences used in the sample preparation are as follows:

Analytical reagent grade reagents  $\text{Bi}_2\text{O}_3$  (99.5%, Himedia),  $\text{Fe}_2\text{O}_3$  (99%, Himedia),  $\text{PbCO}_3$  (99.5%) and  $\text{Nb}_2\text{O}_5$  (99.0%, Himedia) were taken as the initial raw materials in the present work. All the powders were having purity  $\geq 99\%$ . The reacting species in the stoichiometric ratio were thoroughly mixed in an agate mortar-pestle in the presence of AR grade acetone for 2-3 hours. The mixtures were then ball milled (Retsch GmbH & Rheinische, Germany) for 6 hours using zirconia jars and zirconia balls with AR grade acetone as the mixing media.

After proper mixing (hand mixing and ball milling), mixture was kept at least for 12 hours to completely evaporate the acetone which was used during ball milling. The dried powder was gently collected and used for calcinations. The calcinations were carried out in an alumina crucible at different temperature by using globar furnace capable of going up to  $\sim 1600$  K. To study the reaction mechanism for the formation of the BF-0.2PFN solid solutions, ball milled powder were calcined at different temperatures 1053 K, 1073 K, 1113 K, 1123 K, 1133 K, 1143 K and 1148 K for 7 hours. The calcined powder was grind in to fine powders by using an agate mortar and pestle and used for the collection of x-ray diffraction patterns. The x-ray diffraction patterns of  $\text{Bi}_{0.8}\text{Pb}_{0.2}\text{Fe}_{0.9}\text{Nb}_{0.1}\text{O}_3$  powders calcined at different temperatures were recorded as shown in Fig. 1. The x-ray diffraction pattern collected at 1053 K was indexed by using JCPDS files. Since, there were no reflections of ingredient powders  $\text{Bi}_2\text{O}_3$ ,  $\text{Fe}_2\text{O}_3$ ,  $\text{PbCO}_3$  and  $\text{Nb}_2\text{O}_5$  present in XRD patterns, it means reactions were completely taken place. The major components

of XRD pattern has been indexed as a main perovskite peaks of BF-0.2PFN along with two minor's phases of  $\text{Bi}_{36}\text{Fe}_2\text{O}_{57}$  and  $\text{Pb}_3\text{Nb}_4\text{O}_{13}$ . The reflections of the impurity phases  $\text{Bi}_{36}\text{Fe}_2\text{O}_{57}$  and  $\text{Pb}_3\text{Nb}_4\text{O}_{13}$  are indicated by specific symbols as shown in Fig. 1. The small peak located at the  $2\theta \sim 37.5^\circ$  is due to the cell doubling of the main perovskite phase. In order to check the stabilities of the impurity phases, it was calcined at different higher temperatures whose XRD patterns with temperatures are given in the Fig. 1.

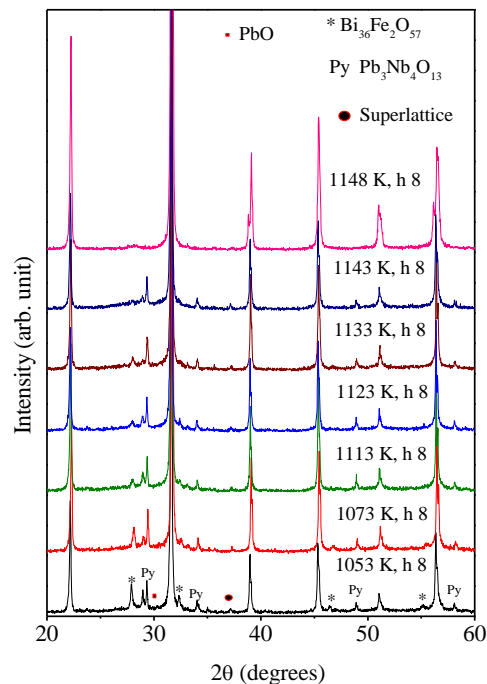


Figure 1. The XRD patterns of calcined  $\text{Bi}_{0.8}\text{Pb}_{0.2}\text{Fe}_{0.9}\text{Nb}_{0.1}\text{O}_3$  powders at different temperatures using  $\text{Bi}_2\text{O}_3$ ,  $\text{Fe}_2\text{O}_3$ ,  $\text{Nb}_2\text{O}_5$  and  $\text{PbCO}_3$  as an ingredients in appropriate molecular ratio.

It was evident from Fig. 1 that as the calcinations temperature was increased intensities of the x-ray peaks corresponding to the impurity phases gradually decreased and completely disappeared at 1158 K. The small hump at  $\sim 28^\circ$  is due to the Bi deficient  $\text{Bi}_2\text{Fe}_4\text{O}_9$  impurity phase which probably starts to appear at sufficiently high calcination temperature. The x-ray diffraction pattern collected at 1148 K was only due to the main perovskite phase of  $\text{Bi}_{0.8}\text{Pb}_{0.2}\text{Fe}_{0.9}\text{Nb}_{0.1}\text{O}_3$  along with superlattice reflections. The superlattice reflections was found in pure  $\text{BiFeO}_3$  and its doped compound because of antiphase rotation of oxygen octahedral along the [111] direction of the perovskite phase. The 1148 K temperature was taken as an optimized calcinations temperature for the  $\text{Bi}_{0.8}\text{Pb}_{0.2}\text{Fe}_{0.9}\text{Nb}_{0.1}\text{O}_3$  composition. For synthesis of insulating  $\text{Bi}_{0.8}\text{Pb}_{0.2}\text{Fe}_{0.9}\text{Nb}_{0.1}\text{O}_3$ , the small trace of  $\text{Li}_2\text{CO}_3$  was mixed in stoichiometric composition before ball milling. The optimized calcinations condition of  $\text{Bi}_{0.8}\text{Pb}_{0.2}\text{Fe}_{0.9}\text{Nb}_{0.1}\text{O}_3$  was taken as initial condition for the calcinations of 1% by weight  $\text{Li}_2\text{CO}_3$  doped  $\text{Bi}_{0.8}\text{Pb}_{0.2}\text{Fe}_{0.9}\text{Nb}_{0.1}\text{O}_3$  composition. The impurities free 1% by weight  $\text{Li}_2\text{CO}_3$  doped  $\text{Bi}_{0.8}\text{Pb}_{0.2}\text{Fe}_{0.9}\text{Nb}_{0.1}\text{O}_3$  composition was successfully calcined at 1140 K.

**2.1 Preparation of Green Pellets and Sintering:** After calcinations, the sample was properly crushed and mixed with an organic binder of 2% polyvinyl alcohol (PVA) solution in an agate mortar. PVA mixed powder was used for the preparation of green pellets. A cylindrical steel die of 12 mm diameter was used to make green pellets of BF-0.2PFN. Initially, the die was kept in a highly viscous mobile oil to prevent it from rusting. After taking out from the oil, the die was cleaned with acetone. Just before putting the powder in the die for pressing, some stearic acid solution was used in the inner surface of the die to avoid sticking of the powder on the inner surface of the die. The  $\text{Bi}_{0.8}\text{Pb}_{0.2}\text{Fe}_{0.9}\text{Nb}_{0.1}\text{O}_3$  powder was put in the die and set in a hydraulic press. Then die containing powder was uniaxially pressed at an optimized pressure (for getting maximum green density) of 65 kN in a hydraulic press. After pellet was formed, it was heated at 773 K for 12 hrs to completely evaporate the binder (PVA). The pellets called as 'green pellets' was kept at 773 K for 12 hours for completely burn-off polyvinyl alcohol before sintering. Sintering was performed in closed alumina crucible with calcined powder of the same composition kept inside the closed crucible as a spacer powder for preventing the loss of  $\text{Bi}^{3+}$  during the sintering. The sintered pellets were then crushed into fine powder. This crushed powder was annealed at 775 K for 12 hours to remove strains which may be developed during the process of crushing.

**3. Results and Discussion:** Fig. 2 depicts room temperature XRD pattern of Li doped  $\text{Bi}_{0.8}\text{Pb}_{0.2}\text{Fe}_{0.9}\text{Nb}_{0.1}\text{O}_3$  composition in  $2\theta$  range of  $20^\circ$ - $70^\circ$ . The small peak at  $2\theta \sim 37^\circ$  confirms the presence of super lattice reflection due to octahedral tilting of R3c phase of BF. The crystal structure analysis using FullProf was also carried out to confirm the crystal structure of Li doped  $\text{Bi}_{0.8}\text{Pb}_{0.2}\text{Fe}_{0.9}\text{Nb}_{0.1}\text{O}_3$  sample. The FullProf analysis confirms the rhombohedral phase with R3c space group for Li doped  $\text{Bi}_{0.8}\text{Pb}_{0.2}\text{Fe}_{0.9}\text{Nb}_{0.1}\text{O}_3$  sample.

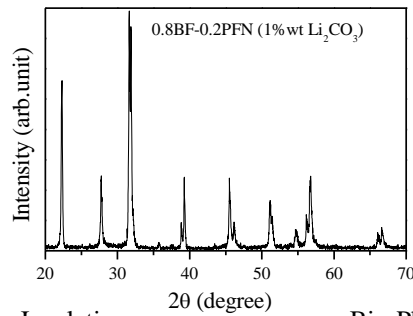


Figure 2. The XRD patterns of Insulating  $\text{Bi}_{0.8}\text{Pb}_{0.2}\text{Fe}_{0.9}\text{Nb}_{0.1}\text{O}_3$  powders. The small amount of  $\text{Li}_2\text{CO}_3$  i.e. approximately 1% by weight of stoichiometric composition of  $\text{Bi}_{0.8}\text{Pb}_{0.2}\text{Fe}_{0.9}\text{Nb}_{0.1}\text{O}_3$  was used before ball milling.

For the dielectric measurements, BF-0.2PFN pellets were smoothly polished with  $0.25\ \mu\text{m}$  diamond paste and then washed with acetone to clean the pellets surface. Isopropyl alcohol was then applied to the polished surface for removing the moisture, if any, on the pellets surface. Fired-on silver paste was subsequently applied on both the faces of the pellets. It was first dried at 423 K in an oven and then cured by firing at 773 K for about 2 min. The temperature dependent dielectric measurements at 1000 Hz were carried out at a heating rate of 1 K/min using a Novo control (Alpha-A) high performance frequency analyzer. Fig. 3 depicts the temperature dependence dielectric plot of  $\text{Bi}_{0.8}\text{Pb}_{0.2}\text{Fe}_{0.9}\text{Nb}_{0.1}\text{O}_3$  at 1 k Hz frequency.

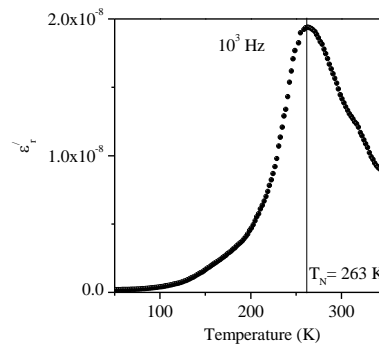


Figure 3. Temperature dependence plot of dielectric constant ( $\epsilon_r$ ) of BF-0.2PFN at 1000 Hz frequency.

The dielectric constant initially increases with increasing the temperature and after making high at antiferromagnetic to paramagnetic transition temperature  $T_N \sim 263\ \text{K}$ , it decreases with increasing temperature. The large peak in dielectric constant at  $T_N \sim 263\ \text{K}$  is due to strong magnetodielectric coupling in BF-0.2PFN sample.

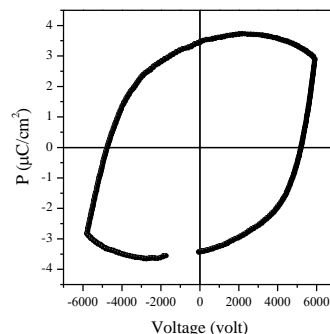


Figure 4. Ferroelectric hysteresis loop measured on insulating  $\text{Bi}_{0.8}\text{Pb}_{0.2}\text{Fe}_{0.9}\text{Nb}_{0.1}\text{O}_3$  pellets.

The huge ferroelectric hysteresis loop is shown in Fig. 4. The remanent polarization  $P_r \sim 3.5\ \mu\text{C}/\text{cm}^2$  is observed.

**4. Conclusion:** The insulating compositions of  $\text{Bi}_{0.8}\text{Pb}_{0.2}\text{Fe}_{0.9}\text{Nb}_{0.1}\text{O}_3$  solid solution was successfully synthesized by solid state reaction method. The synthesized samples were nearly free from all the impurity phases such as  $\text{Bi}_2\text{Fe}_4\text{O}_9$ ,  $\text{Bi}_{25}\text{FeO}_{39}$ ,  $\text{Bi}_{36}\text{Fe}_2\text{O}_{57}$ ,  $\text{Pb}_3\text{Nb}_4\text{O}_{13}$  and  $\text{Pb}_2\text{Nb}_2\text{O}_7$  which are commonly formed during the different stages of synthesis. The ferroelectric hysteresis loop confirms the  $\text{Bi}_{0.8}\text{Pb}_{0.2}\text{Fe}_{0.9}\text{Nb}_{0.1}\text{O}_3$  sample is good insulator.

**5. References:**

1. Fiebig M 2005 J. Phys. D, **38** R123.
2. Ramesh R and Spaldin N A 2007 Nature Mater. **6** 21
3. Cheong S W and Mostovoy M 2007 Nature Material, **6** 13
4. Eerenstein W, Mathur N D and Scott J F 2006 Nature, **442** 759
5. Lebeugle D., Colson D., Forget A., and Viret M. 2007 Appl. Phys. Letters, **91** 022907
6. Catalan G. and Scott J. F. Adv. Mater. 2009 **21** 2463-2485
7. W. Kaczmarek and Z. Pajak, 1975 Solid State Commun. **17**, 807.
8. Y. E. Roginskaya, Y. Y. Tomashpolskii, Y. N. Venevtsev, V. M. Petrov, and G. S. Zhdanov, 1966 Sov. Phys. JETP **23**, 47.
9. I. Sosnowska, M. Loewenhaupt, W. I. F. David, and R. M. Ibberson, 1993 Mater. Sci. Forum **133-136**, 683.
10. Q. Q. Wang, Zhuo Wang, X. Q. Liu, and X.M. Chen, 2012 J. Am. Ceram. Soc. **95**, 670.
11. G. A. Smolenskii and V. M. Yudin, 1965 Sov. Phys.-Solid State **6**, 2936.
12. H. Paik, H.-C. Kim, K. No, Y.-II Kim, D. P. Cann, and J. Hong, 2009 J. Appl. Phys. **105**, 07D919.
13. Kumar, M. M., Palkar, V. R., Srinivas, K. and Suryanarayana, S. V., "Ferroelectricity in a pure BiFeO<sub>3</sub> ceramic," **2000** Appl. Phys. Lett., **76**, 2764.
14. Kumar, M. M., Srinivas, A. and Suryanarayana, S.V., "Structure property relations in BiFeO<sub>3</sub>/BaTiO<sub>3</sub> solid solutions", **2000** J. Appl. Phys., **87**, 855-962.
15. D. Lebeugle, D. Colson, A. Forget, M. Viret, P. Bonville, J. F. Marucco, and S. Fusil, 2007 Phys. Rev. B **76**, 024116.
16. D. Lebeugle, D. Colson, A. Forget, and M. Viret, 2007 Appl. Phys. Lett. **91**, 22907.
17. Pradhan, A. K., Zhang, K., Hunter, D., Dadson, J. B., Loiutts, G. B., Bhattacharya, P., Katiyar, R., Zhang, J., Sellmyer, D. J., Roy, U. N., Cui, Y., and Burger, A., **2005** J. Appl. Phys., **97**, 093903.
18. Lejeune and Boilot J. P., **1982** Ceramic Int. **8**, 99-103.
19. Jenhi M., Ghadraoui E. H., Bali H., Aatmani M. and Rafiq M, **1998** Eur. J. Solid State Inorg. Chem. **35**, 221-230.